Drying of Almonds I: Single Particle

Chilka, A. G., & Ranade, V. V. (2017). Drying of Almonds I: Single Particle. *Indian Chemical Enginer*, 1-23. https://doi.org/10.1080/00194506.2017.1333464

Published in:
Indian Chemical Enginer

Document Version:
Peer reviewed version

Drying of Almonds I: Single Particle

Amarvir G. Chilka[1, 2] and Vivek V. Ranade[*, 3]

[1]Chemical Engineering and Process Development Division
CSIR - National Chemical Laboratory
Pune 411008, INDIA

[2]Academy of Scientific and Innovative Research (AcSIR), CSIR-National Chemical Laboratory (CSIR-NCL) Campus, Pune 411008, INDIA

[3]School of Chemistry and Chemical Engineering, Queen's University Belfast, Belfast BT9 5 AG, UK
*E-mail: V.Ranade@qub.ac.uk

Abstract

Drying is an essential unit operation required in food processing industries, particularly in the dry fruits industry. Drying of almonds exhibit many characteristic features such as non-spherical shape, swelling/ shrinkage as a function of moisture content, uneven drying because of their peculiar shape and proximity to other almond kernels and so on. In this study, we have investigated the drying of almonds through experiments and computational modeling. In this regard, Mettler Toledo Halogen moisture analyzer unit was used to conduct experiments for a single almond kernel. In this widely used equipment, internal air flow patterns and therefore heat and mass transfer depend on natural circulation of air. A detailed three dimensional computational fluid dynamics (CFD) model was used to simulate the air flow pattern, heat and mass transfer in the drying unit. Carefully designed experiments with a single almond kernel were carried out at different temperatures to estimate key parameters of interest (drying kinetics and effective diffusivity). The CFD model was also used to quantify non-uniform heat and mass transfer and therefore non-uniform drying of a single almond kernel. The presented approach, models and results might be useful to improve the performance of drying units in industrial systems. The results and models presented here will also provide a basis for further work on multiple almond kernels and on tray dryer unit.

Keywords: Moisture Analyzer; CFD; Almond drying; Kinetics; Transport processes

1. Introduction

Drying is an indispensable unit operation in many food processing applications. Drying of a variety of food product is carried out to reduce their moisture levels in order to increase the shelf life, reduce the probability of developing fungi and to facilitate further processing to obtain the final product. In particular most of the dry fruits are seasonal in nature, which requires appropriate post-harvest storage for a long duration of time. Therefore it is important to understand the influence of key process

parameters on drying of dry fruits. There are few studies focusing on drying kinetics of dry fruits, Kaya et. al.[1] has studied the convective drying kinetics of kiwi fruit. Togrul et. al.[2] have studied convective drying kinetics of single apricot. Almond is one of the widely cultivated and consumed dry fruit across the globe. It is important to ensure appropriate drying of almonds as more than desirable moisture will increase possibility of developing fungi, and over drying will adversely impact the economics, due to loss of weight.

Critical review of literature did not reveal availability of drying kinetics data for almonds. Taitano et. al.[3] has studied moisture adsorption and thermodynamic properties of California grown almonds. They have reported, variation of diffusivity with respect to temperature, and thermodynamic values for almond kernel. Pearson [4] has studied the effect of temperature (55 °C to 110 °C) on drying of almonds for concealed damage. Pahlevanzadeh and Yazdani [5] have determined equilibrium moisture content of almond kernel at 15 ºC, 55 ºC and 75 ºC. Almond dimensions, geometric mean diameter, density, porosity and other physical properties were measured by Aydin[6], which have been used in the current study. Widely used drying kinetics of various food products have been explained through empirical and semi-empirical models e.g. single parameter Newton model [Ayensu[7]], two parameter Page model [Karathanos et. al.[8]], two-term exponential models [Akpinar et. al.[9], Verma et. al.[10] and Midilli et.al[11]].

As the drying kinetics is influenced by transport processes (heat and mass transfer) in the experimental drying equipment, the afore-mentioned drying kinetics models are not intrinsic in nature. These models depend on flow as well as other transport processes. Therefore it is important to understand the flow and transport processes occurring in the drying equipment used for measuring the drying kinetics in order to translate the results for design and operation of commercial units. In this context it is essential to first obtain effective diffusivity from the measured moisture loss data and use this for developing detailed computational fluid dynamics (CFD) based models. Drying process could be explained more accurately, by using developed CFD models which simulate flow, heat and mass transport. In most of the published studies a constant heat and mass transfer values have been used. However, in real scenarios there could be a considerable variation in these values which needs to be accounted for. Kaya et. al.[1], have shown the variation in heat and mass transfer coefficients for drying of kiwi fruits. In their study two dimensional heat and mass transfer within the kiwi fruit was solved. ElGamal et. al.[12] have coupled convective drying CFD based model with diffusion based drying kinetic model for a single rice kernel. It shows the influence of varying heat and mass transfer coefficients over the moisture variation in the rice kernel. Ranjbaran et. al.[13] have simulated deep-bed paddy drying by using drying kinetic model coupled with CFD simulations. CFD simulations have been extensively used in various drying applications like spray dryer, sprouted bed dryers, tray dryers, fluidized bed dryers etc. Jamaleddine and Ray [14] has provided a detailed review on use of CFD for drying applications.

In this work, the scope is restricted to present detailed CFD model of Mettler Toledo halogen moisture analyzer used for drying of a single almond kernel. The work was then used as a basis for extending the model for simulating drying of multiple almonds which are arranged in the shape of a cuboid (8 particles arranged in [2x2x2] cuboid and 27 particles arranged in [3x3x3] cuboid) as well as drying in a tray dryer.

The present work discusses the following:

- Systematic drying experiments for single almond kernel at three different temperatures i.e. 55 ^{o}C, 65 ^{o}C and 75 ^{o}C; experimental data on moisture content as a function of time
- Experimental data on almond surface and air temperature in the Mettler Toledo unit
- Experimental data on dimensions of almond kernel during the drying process (shrinkage of almonds with moisture content)
- Identifying an appropriate drying kinetics model to describe measured moisture variation with time; estimation of model parameters, effective diffusion coefficient, and activation energy.
- CFD modeling to simulate flow, heat and mass transfer in Mettler Toledo unit.
- Simulated variation of heat and mass transfer coefficients over the almond surface
- Simulated moisture distribution for a single almond kernel (and partial validation by comparing with the experimental data)

This presented experimental data, approach and models will be useful to understand the drying kinetics of almonds in different drying units. The work will provide a firm basis for extending the approach towards drying of multiple almonds and towards simulations of industrial drying units.

2. Experimental

Experiments were conducted using Mettler Toledo Halogen moisture analyzer (excellence plus HX204), to study drying kinetics of single almond kernel. Based on the available data, related to almond drying three different temperatures i.e. 55 ^{o}C, 65 ^{o}C and 75 ^{o}C were selected to conduct experiments. Details of the unit, experimental procedure, estimation of error bars, and processing of experimental data are described in following sections.

2.1 Halogen Moisture Analyzer (HX204)

Mettler Toledo Halogen moisture analyzer excellence plus (HX204) unit is widely used to determine the moisture content of various substances. The unit works on the thermogravimetric principle. The initial weight of the sample is determined at the start of the measurement, followed by heating using halogen radiator. As the sample is being dried the instrument continuously records and displays the weight of the sample. Halogen radiator drying technology is an advancement of the infrared drying method. Halogen radiator has a glass pipe filled with halogen gas as the heating element which provides maximum heating output very quickly. The time required to reach the set temperature in this instrument

is much smaller as compared to the traditional IR-technology. The instrument has gold-plated reflector plates to ensure better distribution of thermal radiation over the entire sample surface.

The details of the halogen moisture analyzer unit used in this study are shown in Figure 1. This instrument allows setting a drying method which requires the set temperature and the switch-off criteria to be specified. The least count of the unit for weight measurement is 1 mg, the data was recorded at an interval of 1s for first one hour of the experiment, for the later period the data recording interval was 5s.

2.2 Materials and Experimental Procedure

Dried almonds (California grown) were obtained from local market. Almonds of similar size and each weighing around 1 gram. were segregated and used for the experiments. Drying experiment was carried using single almond kernel. Almonds were initially dried till the weight was constant (change less than 0.1% in an hour at 120 ^{o}C) to determine the dry weight for each almond. In order to obtain initial high moisture content, each almond was soaked in 100 ml distilled water for a period of eight hours. As almonds surface have wrinkles, soaking the almonds also help to make the surface smooth. Dimensions along the three directional axes were measured before and after each drying experiment. Drying experiments were conducted by specifying the temperature set point of Mettler Toledo drying unit as 55, 65 and 75 ^{o}C. A single almond kernel was dried for a drying period of eight hours. The weight of the sample was displayed in the unit with respect to drying time for each experiment. To study repeatability of measurements and estimation of error bars, each almond kernel was soaked and dried thrice, keeping all the drying parameters constant. Dimensions along the three directional axes, i.e. length, width and thickness were also measured for each almond kernel before and after drying experiment using Vernier caliper having a least count of 0.1mm. These measurements provide data on the shrinkage of almond kernel during the drying process.

2.4 Moisture content, Almond skin temperature, Size Change

Using the sample weight data, moisture content was determined as M_t, where W_t is the weight at a time and W_d is the bone dry weight of the sample.

$$M_t = \frac{W_t - W_d}{W_d} \qquad (1)$$

Experiments were also conducted to measure the almond skin temperature and its surrounding air temperature using K-type thermocouples. Two K-type thermocouples were used one placed at the almond surface, and another in the unit to measure the surrounding air temperature. Location of thermocouples is shown in Figure 2. These measurements were conducted to measure the temperature on almond surface, and surrounding air with respect to the set temperature. Experiments were conducted at all the three selected temperatures. Temperature measurements for set temperature of 65 ^{o}C, was recorded for seven hours of drying time. It was observed that temperature measurements attained

constant values within two hours of drying time. Based on this observation experiments for 55 ^{o}C, and 75 ^{o}C were conducted for two hours only.

During the drying process, size of almond kernel changes as the moisture is reduced, experiments were conducted to study the extent of shrinkage. Size of almond kernel was measured at regular interval of 30 minutes during the first 3 hours of drying. As the drying rate was low interval time was increased to 60 minutes.

2.5 *Processing of acquired moisture data*

Experimentally obtained drying curves were fitted using various thin layer drying models as shown in Table 1. The moisture ratio versus drying time data was fitted using each thin layer model, to estimate the corresponding model parameters. The goodness of fit for each model was determined using statistical parameters R^2 and RMSE.

$$RMSE = \left[\frac{1}{N}\sum_{j=1}^{N}\left(MR_{equ,j} - MR_{exp,j}\right)^2\right]^{1/2} \quad (2)$$

Various published semi-theoretical drying kinetic models like Newton, Page, Two-term exponential, Verma et. al. (1985) and Midilli-Kucuk (2002) were used to fit the data.

Table 1: Various thin-layer drying kinetic model available in literature

Model No.	Model name/ Reference	Model Equation	Parameters	R^2/ RMSE
I	Newton Ayensu (1997)	$MR = exp^{(-kt)}$	k=0.543	0.9165 0.0972
II	Page Karathanos & Belessiotis (1999)	$MR = exp^{(-kt^c)}$	k=0.66, c=0.634	0.9821 0.0342
III	Two term exponential Akpinar et. al. (2003)	$MR = aexp^{(-kt)} + (1-a)exp^{(-kat)}$	a=0.178, k=2.334	0.9506 0.0687
IV	Verma et. al. Verma et. al. (1985)	$MR = aexp^{(-kt)} + (1-a)exp^{(-gt)}$	a=0.319, k=4.104, g=0.287	0.9856 0.0304
V	Midilli-Kucuk Midilli et. al. (2002)	$MR = aexp^{(-kt^c)} + bt$	a=1.113, k=0.74, c=0.463,b=-0.0139	0.9856 0.031

$MR = \frac{M_t - M_e}{M_i - M_e}$, where M_t is moisture at time t, M_i, is initial moisture and M_e is the equilibrium moisture. Equilibrium moisture content for almond kernels has been measured at 15 ^{o}C, 55 ^{o}C and 75 ^{o}C by Pahlevanzadeh and Yazdani[5] and Taitano and Singh[3]. They have showed GAB model as the most suitable one to predict the equilibrium moisture for almond kernel. However, with infrared drying method, sample could be dried till the dry matter. Hence for the sake of analysis moisture ratio is

simplified as: $MR = \frac{M_t}{M_i}$, by considering equilibrium moisture as zero, this approximation has been taken from Togrul[16].

Numerical regression analysis was performed using the SOLVER tool through Microsoft Excel spreadsheet. The SOLVER tool works on the Generalized Reduced Gradient (GRG) method of iteration.

3. Modeling of flow, heat transfer and drying in moisture analyzer

Figure 1 shows the schematic of Mettler Toledo unit used to carry out the experiments. The unit has high accuracy for weight measurements which was found to be 99.99% through in build internal weight calibration of the unit. Air through natural circulation enters and leaves the unit through vent openings located at the top. There are two flat plates on either side and two cylindrical plates on top and bottom, which forms a closed enclosure in the unit. A circular halogen lamp is the heat source to maintain set temperature in the unit. Due to the presence of temperature gradients buoyancy driven flow sets up in the unit. The natural convection flow field within the unit was simulated to study the air flow distribution around the almond kernel. The assumptions to carry out the modeling include: (i) Steady state flow (ii) Variation in size and shape of almond has negligible influence on surrounding air flow patterns (iii) Adiabatic operation (iv) Almond surfaces are impermeable for air flow and (v) There is no heat generation within the almond kernel.

3.1 *Model Equations*

Mass continuity, Momentum, energy and radiation equations were solved to simulate the flow and temperature distribution in the unit. As the major mode of heat transfer from halogen lamp in the unit is radiation. Discrete Ordinate (DO) and Surface-to-surface (S2S) radiation models were used to capture the radiation heat transfer in the unit. Equations are not being reproduced here, as the same could be obtained from [18]. To capture the natural convection flow profile within the unit, air density was modeled using incompressible ideal gas law equation. Steady state analysis is carried out for the flow and heat transfer in the unit, while transient analysis is carried out for the drying simulations.

In built energy equation of Ansys Fluent is used to simulate the unsteady temperature profile inside the almond kernel. Below is the equation used to solve the temperature distribution inside almond kernel:

$$\frac{\partial(T)}{\partial t} = \frac{k}{\rho C_p} \left(\frac{\partial^2 T}{\partial {x_i}^2}\right) \quad (3)$$

User defined scalar (UDS) equation of ANSYS Fluent is used to solve for the moisture content in the almond kernel. UDS equation has an unsteady term, convective flux term and a diffusion term. The primary mode of moisture transfer within the almond kernel is diffusion. Only unsteady and diffusion

terms were considered in the UDS equation. Below is reduced form of UDS equation, where Φ, is the scalar, moisture inside almond kernel.

$$\frac{\partial(\emptyset)}{\partial t} = D_o exp^{\frac{-Ea}{R_g T}} \left(\frac{\partial^2 \emptyset}{\partial {x_i}^2}\right) \quad (4)$$

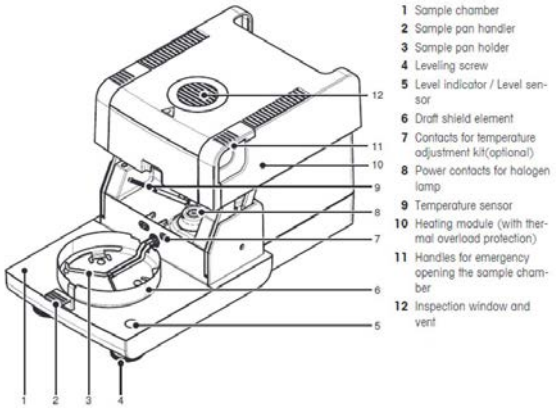

Figure 1. Schematic of Mettler Toledo Halogen moisture analyzer. Source: Operating Instructions manual pg.11.

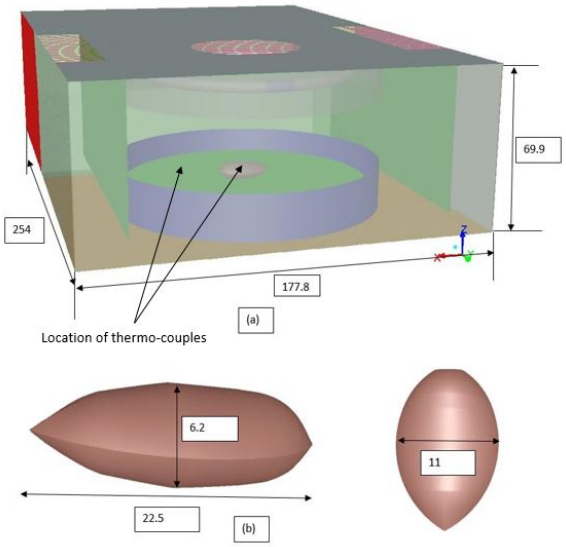

Figure 2. (a) 3D model of unit used for CFD simulations (b) single Almond Kernel model. All dimensions are in mm

3.2 *Boundary and initial conditions*

Heat source for heating is supplied through a cylindrical halogen lamp located in the unit. Halogen lamp surface temperature was set at a constant value, in order to match experimentally measured air temperature.

Thermal properties of almond kernel are reported in Table 2 [Aydin[6], and ASHARE[17]]. Atmospheric pressure value was specified for all the open boundaries of the room region considered.

Table 2: Almond kernel physic-thermal properties

Properties	Value
True Density (Kg/m3)	1000
Thermal Conductivity (W/m-K)	0.2
Specific Heat (J/Kg-K)	2200

For single almond kernel drying simulation, convection boundary type is used for almond surface, with the heat transfer coefficient profiles as obtained from earlier flow simulation and surface temperature corresponding to drying temperature. This modeled the temperature variation within the almond kernel.

Following is the convective boundary condition equation used at the almond surface:

$$\dot{q}_s = h(T_\infty - T) \quad (5)$$

Where h, is heat transfer coefficient profile determined from flow simulations, T_∞, is free stream temperature.

To solver for moisture variation, specified flux boundary type was used for moisture equation, flux was given by:

$$-D_e \left.\frac{\partial m}{\partial n}\right|_s = k_m(M_s - M_a) \quad (6)$$

Where k_m is the mass transfer coefficient determined from flow simulations, M_s is the surface moisture and M_a is the surrounding air moisture content. The initial conditions were:

Temperature: Almond kernel was considered to be at 25 ^oC.

Moisture: Uniform moisture content was specified throughout the almond kernel

3.3 Computational simulations

The first step in computer simulations is to finalize the computational domain and develop appropriate computational mesh for carrying out numerical simulations. For accurate prediction of flow profiles sufficient ambient region surrounding the unit was considered in the computational domain. Computational geometry for the unit was built using all the dimensions of the unit along with the air vent openings located on the top of unit for air circulation. Figure 2 shows the considered geometry of the unit, along with the single almond kernel placed in the unit. Placing the almond kernel in the unit, enables to study the air flow pattern established around the almond kernel. The solid almond kernel was also considered in the analysis for heat transfer.

Fine mesh distribution was maintained around the almond kernel and within the unit, mesh size was gradually increased away from the unit. A boundary layer mesh was generated around the almond kernel surface to resolve the flow and temperature gradients accurately. Combination of hexahedral and tetrahedral cells was used to generate the mesh in the domain. Figure 3 (a) and (b) shows the mesh distribution in the unit and on almond kernel. Very fine triangular cells face mesh was used over almond surface using which boundary layers are added to capture the flow profile around the almond kernel accurately. Meshing size distribution was inline as required for the simulations using laminar model of Ansys Fluent. Very fine tetrahedral cells was used for inside of almond kernel, which is shown in Figure

3 (b). In order to obtain grid independent solution, mesh of three sizes were generated i.e. two, four and seven million cells for the complete computational domain. Mass flow rate of naturally circulated air through the unit was used as one of the parameter to check grid independent solution. The variation in mass flow rate for four and seven million cells simulation results was less than 1%. Hence, four million cells mesh was used for further simulations. Computational geometry was built using Gambit 2.4, a product of ANSYS Inc.

Simulations were carried out using CFD Solver ANSYS Fluent release version 14.5. Second order discretization scheme was used for pressure, momentum, energy and radiation equations. SIMPLE algorithm was used for pressure-velocity coupling. Iterations were carried out till the residuals for all equations were below $1x10^{-5}$. Adequate care was taken to ensure that numerical aspects (number of computational cells, discretization schemes, convergence criteria) do not influence simulated results Ranade[19]. The simulated results are discussed in the following section.

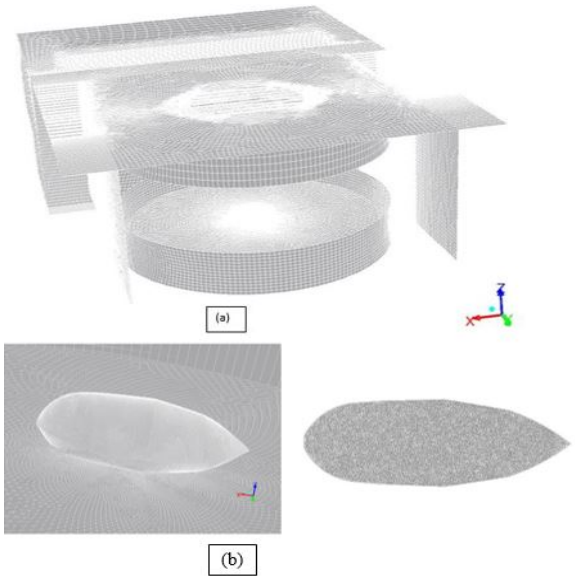

Figure 3. Mesh in the unit (b) Mesh around and inside almond kernel

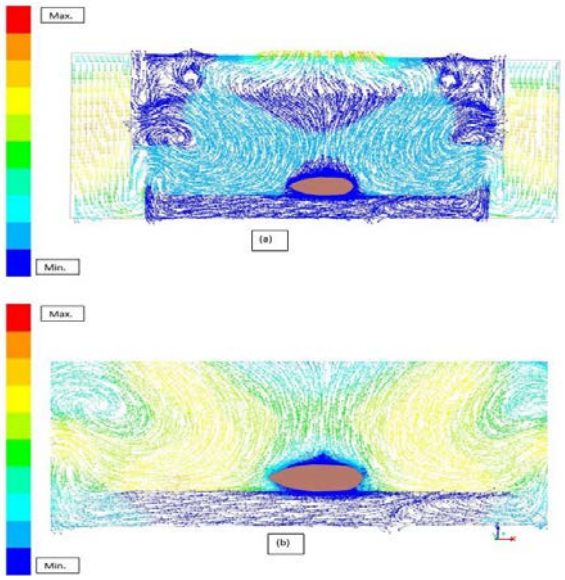

Figure 4. (a) Velocity vectors (cm/s) on a center plane in the unit, Min=0, Max=8 (b) Zoomed view for velocity vectors around almond nut with resuded velocity range, Min=0, Max=2

4. Results and Discussion

CFD simulations generate significant information about flow, heat and mass transfer. To illustrate and discuss these results, here simulated results in the form of velocity vectors and contours of various variables on a plane passing through the center of unit are presented.

4.1 Flow, heat and mass transfer around single almond particle

The objective of these simulations was to understand the air flow pattern and temperature profile in the unit. Air temperature surrounding to almond kernel is validated with the measured values. Figure 4a shows the simulated flow field on a vertical plane passing through the center of unit, for drying set temperature of 65 ^{o}C. It can be seen that the buoyancy driven flow sets up because of non-uniform temperature (density) distribution; flow enters from opening on both sides and exits from the center openings. These results correlate with the experimental observation of hot air leaving from the center openings of the unit and cold air entering unit from side openings. Velocity around the almond unit is rather low (2-3 cm/s). A symmetric flow pattern is established in the unit. As the set temperature is increased the amount of air circulation within the unit is expected to increase due to larger gradient in temperature with respect to surrounding air temperature. This phenomenon is very well captured in the simulations. The simulated values of air flow rates within the unit from the individual openings for all the three temperatures are listed in Table 3. It shows that raising the set point from 55 ^{o}C to 75 ^{o}C leads to 20% increase in net mass flow rate of air through the unit.

Table 3. Mass flow of air through unit at different drying temperatures

Set Temperature (°C)	Mass Flow Rate left slots x10^5 (Kg/s)	Mass Flow Rate left slots x10^5 (Kg/s)	Total Mass Flow Rate x10^5 (Kg/s)
55	1.763	1.719	3.483
65	1.931	1.888	4.3
75	2.35	2.24	4.59

A close-up of flow field around the almond kernel placed in the unit is shown in Figure 4b. It can be seen that there is a significant upward flow from the almond. Thus the natural circulation established in the drying unit ensures that moisture removed from the almond kernel is quickly convected upwards (towards to the outlet). To the best of author's knowledge, the flow field within the Mettler Toledo unit is presented for the first time. The developed CFD model can be used to understand natural convection flow, its dependence on set-point and configuration of the unit (slot shape, size and locations).

Initially radiation heat transfer was modeled using discrete ordinate (DO) radiation model. This model over predicted the almond surface temperature, which led to under prediction of heat and mass transfer coefficients. Using the heat and mass transfer coefficients from DO radiation model, the simulated drying rate of single almond kernel was highly under predicted. Therefore, a surface to surface (S2S) radiation model was used to predict the radiation heat transfer between the halogen lamp and the almond surface. Governing equations for DO as well as S2S models are not included here for the sake of brevity and these may be referred from [18]. Prediction of single almond kernel moisture values using heat and mass transfer coefficients from S2S model were found to agree well with the experimental measurements. Results of S2S radiation model are therefore presented and discussed in this work.

Simulated distribution of temperature field within the drying unit is shown in Figure 5 (a) for the drying set temperature of 65 °C. As the natural convection flow pattern is being established in the unit there is a gradual increase in temperature from the inlet side openings through the unit till outlet center openings. Figure 5 (b) shows the zoomed view of temperature contours around almond kernel. The air temperature around the almond kernel was found to be in the range of 60-65 ^{o}C, and the almond surface temperature was found to be slightly higher (~67 ^{o}C). Experiments were conducted to measure almond surface and the surrounding air temperature within the unit. Measured almond skin temperature was within +/- 0.5 ^{o}C of the set temperature for all the three set points. The temperature of air in the immediate vicinity of the almond was always slightly lower than the set temperature. The measured values are listed in Table 4. It shows that the measured air temperature is about 5 ^{o}C lower than the set-point. The simulated values of temperature at the measurement location are also listed in Table 4. Comparison shows that simulated values agree closely with the measured values.

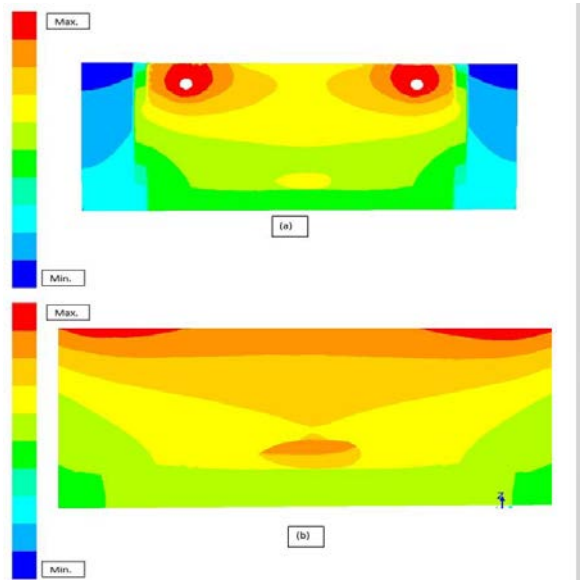

Figure 5. (a) Temperature contours on a center plane in the unit, Min=29 °C, Max=90 °C, (set temperature 65 °C) (b) Zoomed view Min=40 °C, Max= 75 °C, S2S radiation model.

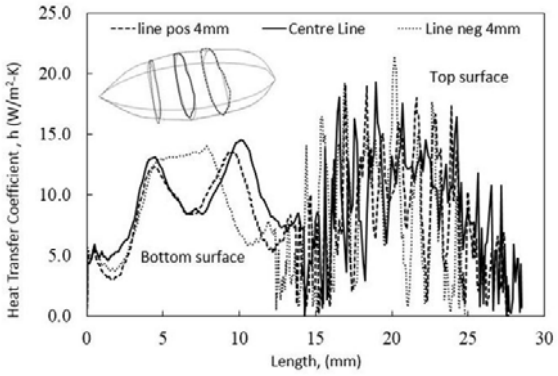

Figure 6. Heat transfer co-efficient profiles at three location on almond surfaces, for set temperature of 65 °C, S2S radiation model

Once the flow field and temperature profile in the unit is established, heat transfer coefficient profile on the almond surfaces was determined using the heat flux equation:

$$-\dot{q}_s = h(T_s - T_\infty) \qquad (7)$$

Where $\dot{q}_s$ is the surface heat flux, T_s is almond surface temperature and T_∞ is the surrounding air temperature. Figure 5 (a) and (b) show there is a temperature distribution of air surrounding almond kernel. A cylindrical volume of 557 cm^3 (diameter 12 cm and height 5 cm) adjacent to the almond kernel was considered to estimate the value of T_∞. Volumetric average air temperature of the cylindrical volume was used for the calculation of heat transfer coefficient profile.

Table 4. Comparison of experimental and CFD predicted air temperatures in the unit

Set Point Temperature (^{o}C)	Air Temperature-Experimental (^{o}C)	Air Temperature-CFD (^{o}C)
55	50	51.5
65	60	62.8
75	70	72

The top almond surface which receives the infra-red radiation of lamp directly and is exposed to upward airflow has the maximum heat transfer coefficient value. As the almond surface has a curvature, central top region has the maximum heat transfer coefficient values. Bottom almond surface has relatively lower values of heat transfer coefficient which is expected. Figure 6 shows the heat transfer coefficient profile along the circumference of the almond at three different axial locations. It could be seen that the values of heat transfer coefficient for the bottom surface is almost 50% lower as compared to that of the top surface. It is also evident from the heat transfer coefficient profiles that it is important to consider a variation in heat transfer coefficient values over the almond surface rather than considering a constant value. This will considerably impact the drying characteristics within the almond kernel. Once the heat transfer coefficient profile is determined, using thermal and concentration boundary layer analogy [20] mass transfer coefficient can be calculated. However this will require the estimation of effective diffusivity, which was obtained using experimentally measured data of moisture content of almond as a function of drying time.

4.2 Analysis of moisture data

Initially multiple drying experiments were conducted to estimate the error bars in the moisture measurements. Experimentally measured moisture values with respect to drying time is shown in Figure 7. This data is helpful to understand the natural variability and error bars of the experimental data. The error bar for the experimental data based on the multiple experiments was in the range of ±5-10%. Drying experiments of single almond kernel were then conducted at three different set point temperatures i.e., 55 ^{o}C, 65 ^{o}C and 75 ^{o}C. Each experiment was conducted in triplicates to ensure repeatability and accuracy of the data. The measured moisture values with respect to drying time for the three set temperature is shown in Figure 8. The initial moisture content of almond kernel is 34%, 28% and 30% for drying temperatures of 55, 65 and 75 ^{o}C respectively. The moisture content at 2 hours

of drying time is 15%, 10% and 8% for drying temperatures of 55, 65 and 75 °C respectively. It takes almost another 6 hours to further reduce the moisture content of almond kernel. This shows the initial drying rate for almond is very high for the first 2-3 hours of drying which decreases considerably for the later stage of drying. Initially moisture transfer occurs from the outer layer of almond kernel.

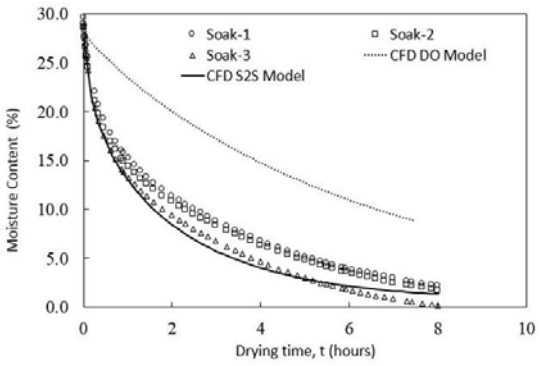

Figure 7. Experimental moisture data for multiple runs and CFD prediction, for set temperature of 65 °C

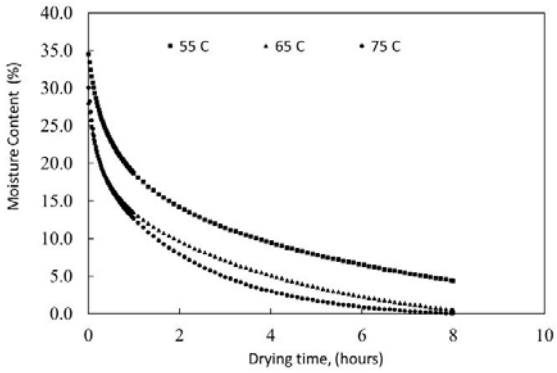

Figure 8. Experimental measured moisture data for three set temperatures of 55 °C, 65 °C and 75 °C

Once the moisture in outer layer is decreased, the diffusion of moisture from the inner core of the kernel to outer surface is essential. The data indicates that in such a later stage, internal diffusion of moisture may control overall drying rate since it appears to be slower than the outside mass transfer coefficient.

The moisture data for almond kernel was fitted using various drying kinetics models available in literature (listed in Table 1). Parameters for each of these models were obtained by numerical regression. Kinetic models IV (Verma et al.) and V (Midilli-Kucuk) appear to predict the moisture pattern of almond reasonably well as compared to other kinetic models (see Table 1). The model of Verma et al. was used to describe the moisture variation at temperatures of 55 °C and 75 °C since it contains lesser number of parameters.

Figure 9 shows the temperature measurements for the almond surface and the surrounding air which was measured experimentally. It shows that within a very short span of time, temperature readings for both the sensors reach constant value.

Almond kernel shrinks slightly during the course of drying. Experiments to measure dimensional change in almond kernel were conducted in triplicates. The total change in dimension was 1.66, 1.86 and 0.54 mm in length, width and thickness respectively. The corresponding percentage reduction in size is 6%, 12% and 6% in length, width and thickness respectively. This data in the normalized form

is shown in Figure 10. As the drying rate is fast for the initial 2 hours, 50% of the total size change happens during this phase of drying.

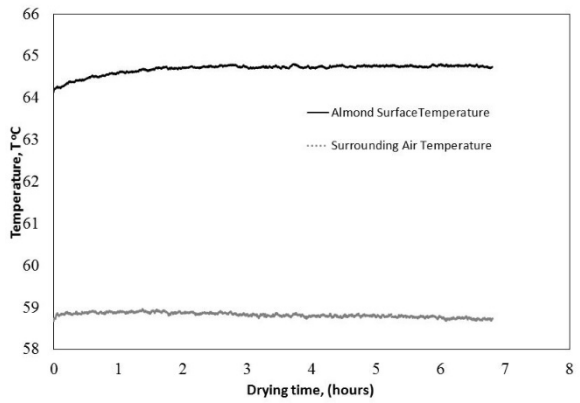

Figure 9. Temperature measurements at almond kernel surface and surrounding air, for set temperature of 65 °C

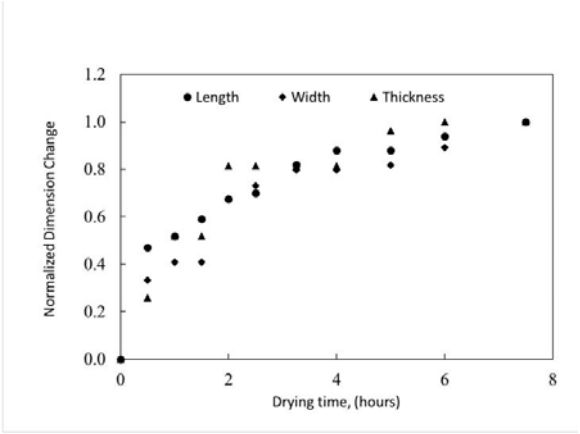

Figure 10. Normalized dimensionless change during the drying process in three directions, dn= (do-di/do-df), Lo=28.34 mm, Lf=26.68 mm; Wo= 15 mm, Wf=13.14 mm; To=8.88 mm, Tf=8.34 mm, for set temperature of 65 °C

Remaining 50% size change happens in the next 6 hours of drying. It is important to understand the extent of shrinkage in a food product during the drying process, which could be accounted in the design of large scale commercial dryers. Certain products like carrot and turmeric has a large variation in size and shape due to the very high (~90% w.b.) initial moisture content. In case of almond kernel, the shape is retained and change in dimension is about 6-12% of the initial dimension having moisture content ~30%.

The moisture data was used to estimate effective diffusivity of almond kernel as discussed in the following section.

Estimation of Effective Diffusivity:

Approximating almond kernel shape by an equivalent sphere, effective diffusivity was estimated using the Fick's second law of diffusion for spherical object as:

$$\frac{\partial m}{\partial t} = D_e \left(\frac{\partial^2 m}{\partial r^2} + \frac{2}{r} \frac{\partial m}{\partial r} \right) \qquad (8)$$

Where r, is the radius of sphere, and m is local moisture content. For constant value of a diffusivity, the analytical solution is [Crank [21]]:

$$MR = \frac{6}{\pi^2} \sum_{n=1}^{\infty} \frac{1}{n^2} \exp\left(-\frac{D_e n^2 \pi^2 t}{r_o^2}\right) \qquad (9)$$

Where r_o is the radius of sphere. Using above solution effective diffusivity for almond kernel was estimated considering the first ten terms of the analytical solution given by equation 7. Nonlinear regression analysis was done using Microsoft Excel tool SOLVER.

Diffusivity is estimated for all the three temperatures at which experiments were conducted. As expected diffusivity value increases with increase in temperature. The observed variation of effective diffusivity with temperature was used to obtain activation energy using the standard Arrhenius law. These diffusivity values are later used to estimate the mass transfer profiles over the almond surface, and predict the moisture distribution within the almond kernel with respect to drying time. Values of effective diffusivity obtained at three temperatures are listed in Table 5. Similar values of diffusivity are reported by Taitano and Singh [3]. The activation energy for almond kernel based on these data was found to be 27.21 KJ/mol.

Table 5. Effective diffusivities for different drying temperatures

Temperature (K)	Effective Diffusivity x10^{10} (m2/s)
328.15	2.67
338.15	3.19
348.15	4.83

Using estimated diffusivity, heat transfer coefficient profile and Lewis number analogy mass transfer coefficient profiles over almond surface are determined. Using the heat and mass transfer profiles drying of single almond particle was simulated.

Estimation of Mass Transfer Coefficient Profiles

Using the heat transfer coefficient profiles on the surfaces of almond kernel mass transfer coefficient profiles was calculated using the analogy between thermal and concentration boundary layers based on the expression given by Chilton and Colburn[20]:

$$k_m = h\left(\frac{DLe^{1/3}}{k}\right) \qquad (10)$$

Le is Lewis number (ratio of thermal diffusivity to mass diffusivity). Higher the Lewis number faster will be heat transfer as compared to mass transfer. For almond kernel Le is around 233. Therefore almond kernel reaches thermal equilibrium very quickly which is also evident from the almond surface temperature measurements. The mass transfer coefficient profiles were used to simulate drying of single almond kernel.

4.3. Drying of single almond kernel

After determination of heat transfer and mass transfer coefficient profiles on almond surface, drying of single almond kernel was simulated. This simulation predict the temperature and moisture distribution within the almond kernel with respect to time. Time dependent simulations were carried out with a time step size of 30s, within each time step 10 iterations were done to ensure internal convergence is achieved within the time step. Care was taken to ensure that simulated results are not influenced by choice of time step or internal iterations. Simulations were carried out till 8 hours of drying time.

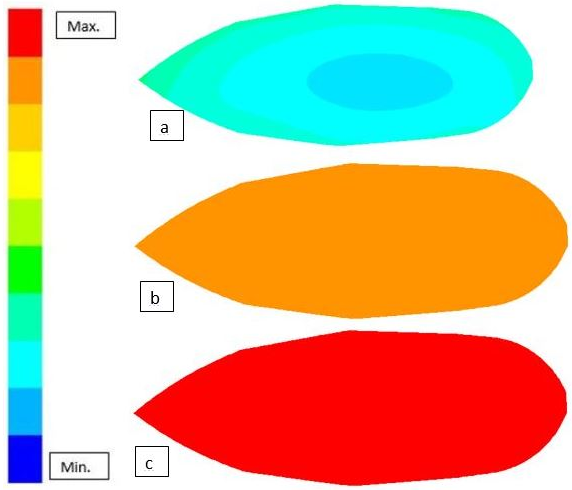

Figure 11. Contours of temperature inside almond kernel during drying process, Min=55 °C , Max=65 °C. (a) Drying time = 30 s, (b) Drying time = 60 s, (c) Drying time = 120 s, Above results are for set temperature of 65 °C, S2S radiation model

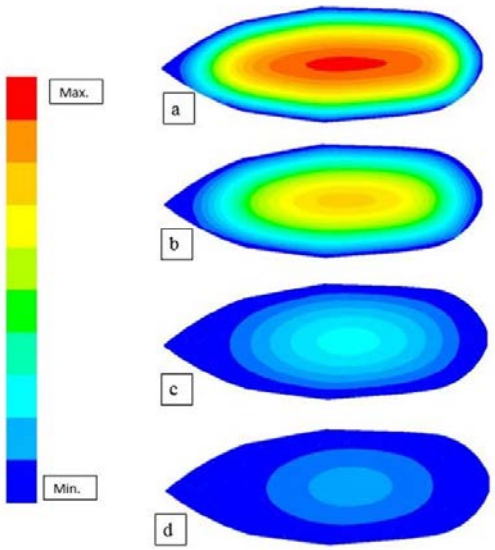

Figure 12. Contours of moisture inside almond kernel during drying process, Min=0.01, Max=0.28. (a) Drying time = 1 hour, Average moisture =0.131, (b) Drying time = 2 hours, Average moisture =0.084, (c) Drying time = 5 hours, Average moisture =0.0288, (d) Drying time = 7 hours, Average moisture =0.013. Above results are for set temperature of 65 °C, S2S radiation model

The simulated variation of the average moisture content of almond kernel for the case with set temperature of 65 ^{o}C is shown in Figure 7 along with the experimental data. Results simulated with two different radiation models (DO and S2S) are included. The DO radiation model is mainly suitable for cases with participating radiation (such as combustion systems). The S2S model is more appropriate

choice for modeling radiative heat transfer in enclosure, without participating media such as the Mettler Toldeo unit considered here. It can be seen that moisture profile predicted by simulation based on S2S model agree well with the experimental data (within experimental error bars). The results confirm that S2S radiation model is more appropriate than the DO model for simulating heat transfer in the Mettler Toledo halogen moisture analyzer unit.

Besides predicting drying of a single almond kernel, CFD models provide significantly more information and insights. For example, the models also allow simulations of internal moisture and temperature distribution (see Figure 11 & 12). The temperature variation is much faster in the almond kernel as compared to the moisture transfer. It can be seen that reduction in moisture content of the region near the surface is much faster than the core. Though this is obvious, CFD models provide quantitative information about such variation. This is especially important when the drying investigations are extended to multiple particles and to commercial drying units. In order to understand influence of neighboring almond kernels on heat and mass transfer and therefore on drying of almond kernel, the CFD model developed here is being extended to multi-particle system (2x2x2 block of eight particles and 3x3x3 block of twenty-seven particles). These studies eventually allow us to build a comprehensive model for large commercial drying units for almond kernels. The approach can be used for other food products as well.

5. Conclusions

In this work flow field and temperature distribution within a Mettler Toledo Halogen Moisture analyzer Excellence Plus (HX204) unit was simulated with the CFD model. Experimental data on drying of a single almond kernel was measured at three different set temperatures, i.e. 55, 65 and 75 ^{o}C. Experimental measurements of temperature were carried out at couple of points. The experimental data on variation of moisture content with time was used to obtain effective drying kinetics. The data was also used to estimate effective diffusivity of almond kernels. The CFD model was also used to simulate variation of heat and mass transfer coefficients around almond kernel. This was then used to simulate moisture variation within the almond kernel. The CFD model was shown to capture variation of the average moisture content of the almond kernel quite well. The key conclusions of the work are:

- The Mettler Toledo HX204 drying unit generated reasonably up flow around the almond kernel placed in the unit by establishing natural convection flow when the set temperature is in the range of 55 to 75 ^{o}C.
- Net mass flow rate increases by 20% when set temperature is increased from 55 ^{o}C to 75 ^{o}C.
- Drying of a single almond kernel can be reasonably described by the drying kinetics models reported by Verma et. al and Middili-Kucuk.

- CFD model based on S2S radiation model was found to capture temperature distribution within the HX204 unit as well as variation of the average moisture content of almond kernel quite well.

The models and approach presented here provide a firm basis for developing tools for simulating large scale drying units for almond kernels.

Nomenclature

Mt	moisture content at time t, Kg/Kg solid (d.b)	MR_{equ}	dimensionless moisture ratio predicted
W_t	weight of almond at time t, kg	MR_{exp}	dimensionless moisture ratio experimental
W_d	bone dry weight of almond, kg	q_s	surface heat flux, W/m2
h	heat transfer coefficient, W/m2-K	T	temperature inside almond kernel, K
T_s	almond surface temperature, K	T_∞	free stream air temperature, K
K_m	mass transfer coefficient, m/s	Le	Lewis number
k	thermal conductivity, W/m-K	C_p	specific heat, J/kg-K
D_e	effective diffusivity m2/s	D_o	Arrhenius constant, m2/s
E_a	Activation energy, KJ/mol	M_s	surface moisture content, Kg/Kg solid
M_a	air moisture content, Kg/Kg dry air	M_e	equilibrium moisture content
RMSE	root mean square error	R^2	coefficient of determination
a,g,k,n	coefficients in thin layer models	r_o	radius of object (m)
R_g	universal gas constant (8314 J/Kmol K)	Φ	user defined scalar
x_i	coordinates	m	moisture content (Kg/Kg)
n	normal to surface	N	number of sample points
t	time (s)	ρ	density (Kg/m^3)

Acknowledgements

The authors are grateful for financial support of this work by CSIR through Indus MAGIC (Innovate, develop and up-scale modular, agile, intensified and continuous processes) project [CSC 123]. The authors also gratefully acknowledge the help from Mr. Yogesh Suryawanshi in the experimental part.

References

1. Kaya, A.; Aydin, O.,; Dincer, I. Experimental and numerical investigation of heat and mass transfer during drying of Hayward kiwi fruits. Journal of Food Engineering **2008,** 88, 323-330
2. Togrul, I.T., Pehlivan, D. Modeling of drying kinetics of single apricot. Journal of Food Engineering **2003**, 58, 23–32
3. Taitano Li Z., Singh R.P., Moisture Adsorption and Thermodynamic Properties of California Grown Almonds (Varieties: Nonpareil and Monterey). International Journal of Food Studies **2012**, 1, 61-75
4. Pearson, T.C., Spectral properties and effect of drying temperature on almonds with concealed damage. Lebensmittel-Wissenschaft und-Technologie **1999**, 32 67-72.
5. Pahlevanzadeh, H.; Yazdani, M. Moisture Adsorption Isotherms and Isosteric Energy For Almond, Journal of Food Process Engineering **2005**, 28, 331-345
6. Aydin, C., Physical properties of almond nut and kernel, Journal of Food Engineering, **2003**, 60, 315-320
7. Ayensu, A. Dehydration of food corps using a solar dryer with convective heat flow, Solar Energy **1997**, 59 121-126
8. Karathanos, V.T., Belessiotis, V.G. Application of a thin layer equation to drying data of fresh and semi-dried fruits. Journal of Agricultural Engineering Research **1999**, 74, 355-361
9. Akpinar, E.K., Bicer, Y., Yildiz, C., Thin layer drying of red pepper. Journal of Food Engineering **2003**, 59, 99–104.
10. Verma, L.R., Bucklin, R.A., Endan, J.B., Wratten, F.T. Effects of drying air parameters on rice drying models. Transactions of the ASAE **1985**, 28, 296–301
11. Midilli, A., Kucuk, H., Yapar, Z. A new model for single layer drying. Drying Technology **2002**, 20 (7), 1503–1513
12. ElGamal, R.; Ronsse, F.; Radwan, S.M; Pieters, J. G. Coupling CFD and Diffusion Models for Analyzing the Convective Drying Behavior of a Single Rice Kernel, Drying Technology **2014**, 32 311-320
13. Ranjbaran, M., Emaid, B., Zare, D., CFD Simulation of Deep-Bed Paddy Drying Process and Performance. Drying Technology **2014**, 32, 919-934
14. Jamaleddine, T.J., Ray, M.B. Application of Computational Fluid Dynamics for Simulation of Drying Proceses: A Review. Drying Technology **2010**, 28, 120-154

15. Operating Instructions Manual for Moisture Analyzer Excellence Plus HX204, Mettler Toledo
16. Togrul, H. Suitable drying model for infrared drying of carrot. Journal of Food Engineering **2006**, 77, 610-619
17. ASHARE Handbook-Refrigeration SI 2006
18. Ansys® Ansys Fluent-Solver v 14.5, Theory Guide
19. Ranade, V.V., Computational flow modeling for chemical reactor engineering, Academic Press, London. **2002**
20. Chilton, T.H,; colburn, A.P. Mass Transfer (absorption) coefficients: prediction from data on heat transfer and fluid friction. Industrial & Engineering Chemistry **1934**, 26(11), 1183-1187.
21. Crank, J. The mathematics of diffusion, Clarendon Press-Oxford, Second Edition **1975**